5-1-2019

Depletion of Myo/Nog Cells in the Lens Mitigates Posterior Capsule Opacification in Rabbits.

Jacquelyn Gerhart
Philadelphia College of Osteopathic Medicine, jacquelynge@pcom.edu

Liliana Werner

Nick Mamalis

Joseph Infanti
Philadelphia College of Osteopathic Medicine, josephin@pcom.edu

Colleen Withers
Philadelphia College of Osteopathic Medicine

See next page for additional authors

Authors
Jacquelyn Gerhart, Liliana Werner, Nick Mamalis, Joseph Infanti, Colleen Withers, Fathma Abdalla, Colby Gerhart, Arturo Bravo Nuevo, Olivia Gerhart, Lori Getts, Kelly Rhodes, Jessica Bowers, Robert Getts, and Mindy George-Weinstein

Depletion of Myo/Nog Cells in the Lens Mitigates Posterior Capsule Opacification in Rabbits

Jacquelyn Gerhart,[1] Liliana Werner,[2] Nick Mamalis,[2] Joseph Infanti,[1] Colleen Withers,[1] Fathma Abdalla,[1] Colby Gerhart,[1] Arturo Bravo-Nuevo,[1] Olivia Gerhart,[1] Lori Getts,[3] Kelly Rhodes,[3] Jessica Bowers,[3] Robert Getts,[3] and Mindy George-Weinstein[1]

[1]Philadelphia College of Osteopathic Medicine, Philadelphia, Pennsylvania, United States
[2]John A. Moran Eye Center, University of Utah, Salt Lake City, Utah, United States
[3]Genisphere, LLC, Hatfield, Pennsylvania, United States

Correspondence: Mindy George-Weinstein, Philadelphia College of Osteopathic Medicine, 4190 City Avenue, Philadelphia, PA 19131, USA;
mindygw@pcom.edu.

RG and MG-W contributed equally to the work presented here and should therefore be regarded as equivalent authors.

Submitted: January 23, 2019
Accepted: March 4, 2019

Citation: Gerhart J, Werner L, Mamalis N, et al. Depletion of Myo/Nog cells in the lens mitigates posterior capsule opacification in rabbits. *Invest Ophthalmol Vis Sci*. 2019;60:1813–1823. https://doi.org/10.1167/iovs.19-26713

Purpose. Posterior capsule opacification (PCO) is a vision-impairing disease that occurs in some adults and most children after cataract surgery. Contractile myofibroblasts contribute to PCO by producing wrinkles in the lens capsule that scatter light. Myofibroblasts in the lens originate from Myo/Nog cells named for their expression of the MyoD transcription factor and bone morphogenetic protein inhibitor noggin. In this study we tested the effects of depleting Myo/Nog cells on development of PCO.

Methods. Myo/Nog cells were eliminated by injecting the G8 antibody conjugated to 3DNA nanocarriers for the cytotoxin doxorubicin (G8:3DNA:Dox) during cataract surgery in rabbits. The severity of PCO was scored by slit lamp analysis, gross and histologic observation, and immunofluorescence localization of α-smooth muscle actin.

Results. G8:3DNA:Dox specifically induced cell death in Myo/Nog cells in the lens. None of the lenses administered G8:3DNA containing 9 to 36 μM doxorubicin developed greater than trace levels of central PCO and few myofibroblasts were present on the capsule. Less than 9% of these lenses exhibited greater than mild levels of peripheral PCO. Doxorubucin itself reduced PCO; however, myofibroblasts and wrinkles were abundant in the lens, and off-target effects were observed in the ciliary processes and cornea.

Conclusions. Myo/Nog cells are the primary source of myofibroblasts in the lens after cataract surgery. Targeted depletion of Myo/Nog cells has potential for preventing PCO and preserving vision.

Keywords: Myo/Nog, posterior capsule opacification, myofibroblasts

Cataracts are opacifications of the lens that may be present at birth or develop with aging in response to prolonged exposure to sunlight, smoking, diabetes, or surgery for other ocular diseases.[1] They are the leading cause of visual impairment and blindness worldwide.[2,3] The World Health Organization estimates that by 2020, 32 million cataract operations will be performed each year. Removal of cataract tissue restores vision; however, 20% to 40% of adults and most children develop a reopacification of the lens, called posterior capsule opacification (PCO), within 3 years of surgery.[4–9] The incidence of PCO continues to rise as the patient ages, such that everyone who undergoes cataract surgery is predicted to require further treatment to improve vision.[6,8,10,11]

Most patients with PCO are treated with neodymium-doped yttrium aluminum garnet laser to clear the lens. While this procedure is effective for most patients, laser therapy is not available worldwide, often has to be repeated, and is estimated to cost health care providers hundreds of millions of dollars a year.[6,12] Some patients develop complications from laser treatment, including retinal detachment and gliosis, macular edema, and glaucoma that further compromise vision and escalate health care costs.[8,10–12] Currently, there is no method for preventing PCO and eradication of the condition remains an unmet goal in ophthalmology.

PCO results from abnormal cellular responses to cataract surgery.[8,13,14] In the regenerative form of PCO, epithelial cells remaining in the lens form masses of differentiating cells called Elschnig pearls and Soemmering's rings.[8,13,15] Both pearls and rings may affect vision depending on their size and location along the visual axis. Lens epithelial cells also may undergo an epithelial to mesenchymal transition and populate the normally cell-free posterior capsule in response to wounding.[8,13,16] In this process, called fibrotic PCO, an abnormal amount of extracellular matrix is deposited on the capsule. A similar phenomenon may occur on the anterior capsule (anterior capsule opacification, ACO). One feature of fibrotic PCO and ACO that significantly contributes to a decline in visual acuity is wrinkling of the capsule by contractile myofibroblasts.[13,16,17] Lens epithelial cells that have transitioned to a mesenchymal phenotype synthesize the myofibroblast marker α-smooth muscle actin (α-SMA).[16,18–20] However, knockdown of α-SMA in cultures of human lens cells does not inhibit matrix contraction, suggesting that other muscle proteins such as myosin may mediate contraction in this system.[21]

We discovered a distinct population of myogenic cells within the lens, called Myo/Nog cells, named for their expression of the skeletal muscle–specific transcription factor MyoD and the bone morphogenetic protein (BMP) inhibitor

Table 1. Doses of G8 mAb, 3DNA, and Doxorubicin Injected Into the Lens and Number of Eyes Evaluated at 1, 2, and 28 Days Following Cataract Surgery

				No. Eyes		
	G8 mAb, μg/mL	3DNA, μg/mL	Dox, μM	Day 1	Day 2	Day 28
BSS	0	0	0	2	2	15
G8:3DNA	152	70	0	1	0	6
3DNA:Dox	0	70	36	1	0	6
G8:3DNA:Dox	1.52	0.7	0.36	1	0	5
	7.6	3.5	1.8	1	0	6
	15.2	7	3.6	0	0	3
	38	17.5	9	0	2	5
	76	35	18	0	2	5
	152	70	36	2	2	12
Dox	0	0	9	0	2	5
	0	0	18	0	2	5
	0	0	36	2	2	8

Eyes were injected with BSS or drugs after insertion of the IOL and before suturing. Eyes were evaluated by gross observation and histologically 1, 2, or 28 days postoperatively. Slit lamp examinations were performed on day 28.

noggin.[22–24] Myo/Nog cells were first identified in the blastocyst of the chick embryo.[22,25,26] During gastrulation, they are distributed in low numbers throughout the embryo, including the eyes.[24,27,28] Stable transcription of both genes, regardless of their environment, ensures that Myo/Nog cells remain committed to the skeletal muscle lineage and serve as essential regulators of BMP signaling.[24,27–29] Elimination of Myo/Nog cells in the blastocyst results in hyperactive BMP signaling and severe malformations, including eye defects ranging from anophthalmia to lens dysgenesis and overgrowth of the retina.[24,28,30]

Myo/Nog cells also react to wounding in the embryo and adult.[30–37] Within 24 hours of epidermal abrasion, Myo/Nog cells increase in number and populate the wound.[38] In the retina, the Myo/Nog population expands in response to hypoxia and damaging levels of light.[34,35] Depletion of Myo/Nog cells in the mouse model of retinopathy of prematurity results in an increase in photoreceptor cell death, and their addition to the vitreous following light damage reduces cell death and improves visual performance.[34,35]

While Myo/Nog cells are neuroprotective in the retina, their wound-healing response in the lens may be detrimental to vision. In the human lens, Myo/Nog cells surround wounds, synthesize α-SMA and skeletal muscle proteins, and overlie wrinkles in the capsule.[32,33] Depletion of Myo/Nog cells with the targeting G8 monoclonal antibody (mAb) bound to complement or conjugated to two-layered 3DNA nanocarriers intercalated with the cytotoxin doxorubicin (G8:3DNA:Dox) prevents the emergence of myofibroblasts in response to wounding in explant cultures of chick embryo and human anterior lens tissue.[32,33,37]

The behavior of Myo/Nog cells in the lens in vivo has been studied in rabbits. Within 24 hours of cataract surgery, their number was significantly elevated in the lens, ciliary body, and cornea.[36] Myo/Nog cells also have been found on the zonules of Zinn, apparently migrating between the ciliary processes and lens[36] (Gerhart JV, et al. *IOVS* 2017;58:ARVO E-Abstract 3635). One month after surgery, Myo/Nog cells are present on the internal and external surfaces of the posterior capsule; express α-SMA, MyoD, and striated muscle myosin; and overlay wrinkles in the capsule.[36] In this report, we describe the effect of depleting Myo/Nog cells on the development of PCO following cataract surgery in rabbits.

Methods

Cataract Surgery

Cataract surgery was performed on New Zealand white, female rabbits weighing between 2.8 and 3.2 kg as described previously.[38–40] Details of surgery are provided in the Supplementary Material. All procedures adhered to the ARVO Statement for the Use of Animals in Ophthalmic and Vision Research.

Drug Treatment

A total of 900 μL balanced salt solution (BSS) or drugs diluted in BSS was injected behind and in front of the intraocular lens (IOL). Drug treatments consisted of purified G8 IgM mAb conjugated to two-layered 3DNA nanocarriers (Genisphere, LLC, Hatfield, PA, USA) (G8:3DNA), doxorubicin (Dox) (Sigma-Aldrich, St. Louis, MO, USA), 3DNA intercalated with doxorubicin (3DNA:Dox), G8:3DNA intercalated with Dox (G8:3DNA:Dox), and 3DNA:Dox. Synthesis of 3DNA, conjugation to the G8 mAb, maintenance of functional binding activity, and internalization has been described previously.[33] The amounts of G8 mAb, 3DNA, and Dox for each dose are listed in Table 1.

Gross and Histologic Analyses of the Anterior Segment

Eyes were examined grossly the first 2 days after surgery for untoward effects, including inflammation, bleeding, and corneal edema. The number of eyes obtained at 1, 2, and 28 days is indicated in Table 1. Globes were bisected coronally just anteriorly to the equator. Gross examination and photographs from the posterior aspect (Miyake-Apple view) were performed to score (1) central PCO (3 mm behind the optic), (2) peripheral PCO (extending from the optic-haptic junction posteriorly), (3) ACO, (4) intensity and area of Soemmering's rings, and (5) IOL decentration and fixation.[41,42] Capsular bags were observed for epithelial outgrowth, fibrosis, capsular wrinkling, Elschnig pearls, and fibrin deposits. Tissue was embedded in paraffin, sectioned at 10 μm, and stained with hematoxylin-eosin (H&E). Five sections from each eye were evaluated for the extent of PCO and ACO, noting the presence

of proliferative cortical material, pearls and fibrous metaplasia, openness of the trabecular meshwork, and morphology of the ciliary body, cornea, and peripheral retina.

Evaluation of the Anterior Segment by Slit Lamp Examination

Slit lamp examinations were performed weekly as described previously.[41,43] A scoring system of 0 (none observed), 1 (trace), 2 (mild), 3 (moderate), and 4 (severe) was used to evaluate the anterior segments for (1) conjunctival injection (redness) and discharge, (2) appearance of the limbal and iris vasculatures, (3) corneal opacity/edema, (4) cellularity and flare of the aqueous humor, (5) IOL centration, (6) posterior synechia (adhesion of the iris to the anterior lens), (7) inflammatory deposits, (8) ACO (area of the anterior capsule in front of the anterior optic surface of the intraocular lens), and (9) PCO (area of the posterior capsule behind the IOL). Retroillumination images with the pupil fully dilated were obtained for documentation of lens opacification and fibrosis.

Immunofluorescence Localization

Paraffin-embedded tissue sections of the anterior segment were labeled with fluorescent antibodies as described previously.[22,24,29] Sections were incubated with the G8 IgM mouse mAb[29] or G8 and an mAb to α-SMA directly conjugated with fluorescein (Sigma-Aldrich). G8 was visualized with affinity-purified, F(ab')2 goat anti-mouse IgM μ chain conjugated with rhodamine (Jackson ImmunoResearch, West Grove, PA, USA). Nuclei were labeled with Hoechst dye. Background fluorescence was assessed by incubating tissue sections with secondary antibodies alone. Sections also were colabeled with G8 and fluorescent terminal deoxynucleotidyl transferase–dUTP nick-end labeling (TUNEL) reagents (Roche Diagnostics, Mannheim, Germany) to detect cell death.[30,32]

Antibody labeling was analyzed with the Nikon Eclipse E800 epifluorescence microscope (Nikon Instruments Inc., Melville, NY, USA) equipped with the Evolution QE Optronics video camera and Image Pro Plus image analysis software program (Media Cybernetics, Rockville, MD, USA). Figures were annotated and adjusted for brightness and contrast with Adobe Photoshop CC 2014 (Adobe Inc., San Jose, CA, USA).

Observational and Statistical Analyses

All analyses were performed while blinded to treatment. Treatment groups were analyzed for differences in means by analysis of variance. The Tukey's test was used for pairwise comparisons. Treatment groups failing to exhibit normality with the Shapiro-Wilk test were analyzed by the Kruskall-Wallace test followed by pairwise comparisons with the Dunn's test. Significant differences/*P* values were calculated with a 95% confidence interval.

Results

Effects of Drug Treatment on the Anterior Segment 24 to 48 Hours After Cataract Surgery

Eyes either appeared normal or exhibited mild corneal edema located superiorly within the incision site on the first and second day after surgery (Fig. 1). Both eyes that received 36 μM Dox and one eye administered 18 μM Dox showed signs of corneal edema and attenuation of the endothelium (Fig. 1).

No cell death was revealed with TUNEL staining in lenses administered BSS, 36 μM Dox, or 3DNA:Dox the day after surgery, whereas all G8+ cells were TUNEL+ with the highest dose of G8:3DNA:Dox 24 hours after surgery (not shown). The results of TUNEL staining 2 days after surgery are displayed in Figure 1 and Table 2. Fewer G8+/TUNEL− cells were present in lenses injected with G8:3DNA:Dox than BSS, reaching significance with the 18-μM dose. No G8+/TUNEL+ cells were observed in BSS-treated lens. G8+ cells were dying in lenses administered either G8:3DNA:Dox or Dox. The number of G8+/TUNEL+ cells was significantly lower in lenses treated with 36 μm than 18 μm G8:3DNA:Dox, possibly reflecting a loss of dead cells between 24 and 48 hours of treatment. Lenses with all three doses of Dox had significantly more G8−/TUNEL+ cells than those with the highest dose of G8:3DNA:Dox.

In the ciliary processes, the number of G8+/TUNEL− cells was similar in all treatment groups (Table 2). No dying G8+ cells were observed in this structure after administration of G8:3DNA:Dox and few were dying in response to Dox. However, significantly more G8−/TUNEL+ cells were present in the ciliary processes with the two highest doses of Dox than those administered any dose of G8:3DNA:Dox (Fig. 1; Table 2).

No G8+ cells appeared to be dying in the cornea following treatment with BSS or any dose of G8:3DNA:Dox (Fig. 1; Table 2). Significantly more G8+/TUNEL+ cells were observed with the highest dose of Dox than BSS and all three doses of G8:3DNA:Dox (Table 2). The number of G8−/TUNEL+ cells also was significantly higher in the cornea of eyes administered the highest dose of Dox than the two highest doses of G8:3DNA:Dox.

These results demonstrate that G8:3DNA:Dox induces cell death in Myo/Nog cells of the lens. Very few G8+/TUNEL− cells remained in the lens 2 days following drug treatment. The lack of significant differences between the number of G8−/TUNEL+ cells in the lens in response to BSS versus G8:3DNA:Dox suggests that the drug specifically targets Myo/Nog cells. By contrast, Dox kills Myo/Nog and lens epithelial cells and has off-target effects in the ciliary body and cornea.

Effect of Drug Treatment on the Development of PCO

PCO was not visible by slit lamp examination 1 week postoperatively. Trace levels of PCO (scores of 0.5–1) beginning at the optic-haptic junction were visible in some lenses in all treatment groups 2 weeks after surgery except those administered 3.6 μM G8:3DNA:Dox (Supplementary Table S1). By week 3, PCO had progressed from trace to mild in all treatment groups except lenses injected with 3.6 to 36 μM G8:3DNA:Dox, 9 to 36 μM Dox, and 36 μM 3DNA:Dox (Supplementary Table S1).

Photographs of slit lamp examinations at week 4 are displayed in Supplementary Fig. S1. Whereas 80% to 100% of lenses injected with BSS and G8:3DNA had developed mild to severe PCO, only 20% to 33% of lenses given the two highest doses of G8:3DNA:Dox had greater than trace levels of PCO on week 4 (Table 3). No PCO was observed in 20% to 40% of the lenses treated with the two highest concentrations of G8:3DNA:Dox and Dox. The percentage of lenses with greater than trace levels of PCO also was reduced after treatment with comparable doses of Dox or 3DNA:Dox (17%–40%). None of the lenses treated with G8:3DNA:Dox, Dox, or 3DNA:Dox had severe PCO. A downward trend in the mean PCO scores was observed from BSS and G8:3DNA to the three highest doses of G8:3DNA:Dox, Dox, and 3DNA:Dox, although significant differences were not found between the treatment groups (Supplementary Fig. S2A).

The effect of drug treatment on central and peripheral PCO was evaluated on week 4 by gross observation (Table 3).

Investigative Ophthalmology & Visual Science

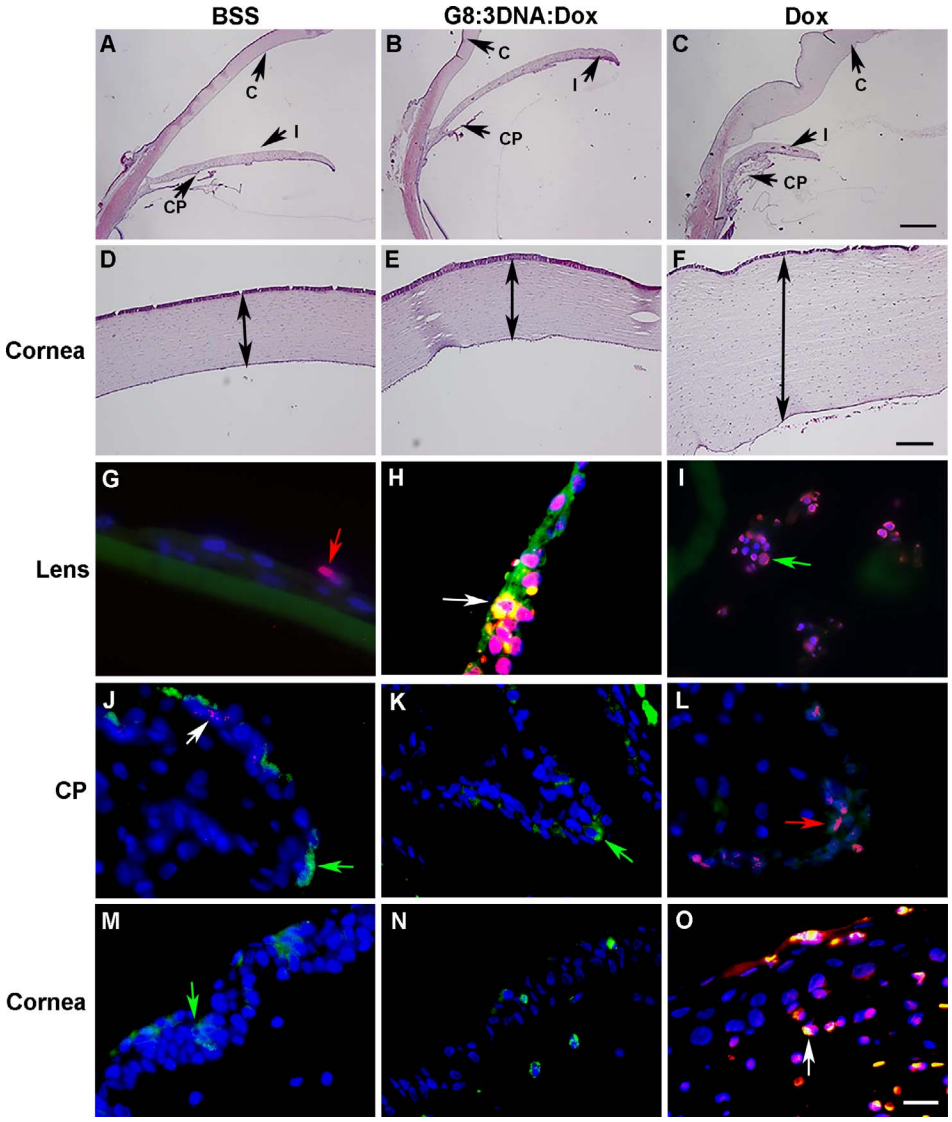

Figure 1. Effects of drug treatment 2 days after cataract surgery. Lenses were injected with BSS or 36 μM G8:3DNA:Dox or Dox during cataract surgery. Two days later, tissue sections were stained with H&E (**A–F**) or double labeled with the G8 mAb (*green*) and TUNEL reagents (*red*) (**G–O**). Overlap of *red* and *green* appears *yellow* in merged images. Nuclei were labeled with Hoechst dye (*blue*). *White arrows* = G8+/TUNEL+ cells; *green arrows* = G8+/TUNEL– cells; *red arrows* = G8–/TUNEL+ cells. *Bar*: 270 μM in (**A–C**), 54 μM in (**D–F**), and 9 μM in (**G–O**). C, cornea; CP, ciliary processes; I, iris.

Whereas 33% to 53% of lenses treated with BSS or G8:3DNA had mild to severe central PCO, no central PCO was found in 40% to 63% of lenses treated with the two highest doses of G8:3DNA:Dox. None of the lenses administered the three highest doses of G8:3DNA:Dox, two highest doses of Dox, or 3DNA:Dox had developed greater than trace levels of central PCO. The mean central PCO scores were higher for BSS- and G8:3DNA-treated lenses than 3.6 to 36 μM G8:3DNA:Dox, 9 to 36 μM Dox, and 3DNA:Dox (Supplementary Fig. S2B). A significantly higher PCO score was found for 1.8 μM G8:3DNA:Dox than the two highest doses of this drug and highest dose of Dox.

Whereas 83% to 100% of lenses treated with BSS, G8:3DNA, and the three lowest doses of G8:3DNA:Dox had developed mild to severe peripheral PCO, no peripheral PCO had developed in 20% to 40% of lenses administered the two highest doses of G8:3DNA:Dox and Dox, and 3DNA:Dox (Table 3). Only 16% to 20% and 25% to 40% of lenses treated with the two highest concentrations of G8:3DNA:Dox and Dox, respectively, had greater than trace levels of peripheral PCO. None of the lenses administered 9 and 18 μM G8:3DNA:Dox, or 18 μM Dox, had moderate to severe peripheral PCO. The mean peripheral PCO scores of the three highest doses of G8:3DNA:Dox and Dox were lower than the means of BSS, G8:3DNA, and low doses of G8:3DNA:Dox (Supplementary Fig. S2C). BSS-treated lenses had significantly greater peripheral PCO than the two highest doses of G8:3DNA:Dox and highest dose of Dox. Significant differences also were observed between low doses of G8:3DNA:Dox and high doses of G8:3DNA:Dox, Dox, and 3DNA:Dox.

These analyses demonstrated that G8:3DNA:Dox, Dox, and 3DNA:Dox prevent or reduce the severity of PCO as measured by slit lamp analysis. Central PCO was inhibited to a greater extent than peripheral PCO. However, in both areas of the capsule, most lenses treated with the higher doses of G8:3DNA:Dox and Dox had only trace or no PCO.

Table 2. Cell Death in the Anterior Segment 2 Days Following Cataract Surgery

	No. Eyes	No. Sect*	Lens†			CP‡			Cornea§		
			G8+/TUN−	G8+/TUN+	G8−/TUN+	G8+/TUN−	G8+/TUN+	G8−/TUN+	G8+/TUN−	G8+/TUN+	G8−/TUN+
BSS	2	10	5 ± 3	0	2 ± 2	11 ± 7	0.4 ± 1	4 ± 2	6 ± 4	0	5 ± 1
G8:3DNA:Dox											
9 μM	2	8	1 ± 1	4 ± 5	2 ± 3	8 ± 3	0	1 ± 2	6 ± 4	0	3 ± 4
18 μM	2	9	0.2 ± 0.4	5 ± 5	0.4 ± 1	10 ± 6	0	1 ± 1	19 ± 10	0	3 ± 4
36 μM	2	8‖	1 ± 2	2 ± 4	0.3 ± 1	7 ± 4	0	0.2 ± 1	6 ± 3	0	2 ± 4
Dox											
9 μM	2	9	2 ± 2	1 ± 1	6 ± 11	8 ± 4	2 ± 4	9 ± 6¶	12 ± 8	3 ± 9	42 ± 39¶
18 μM	2	11	2 ± 2	5 ± 3	9 ± 5	10 ± 6	2 ± 4	9 ± 6	13 ± 5	1 ± 1	34 ± 22
36 μM	2	7	3 ± 4	5 ± 4	13 ± 8	10 ± 8	3 ± 5	14 ± 2#	9 ± 9	6 ± 5	61 ± 31#

* Tissue sections (Sect) were double labeled with the G8 mAb and TUNEL (TUN) reagents to detect cell death. The results are the mean ± standard deviation of the number of cells in the lens, ciliary processes (CP), and cornea labeled for G8 only (G8+/TUN−), both G8 and TUNEL (G8+/TUN+), or TUNEL only (G8−/TUN+).

† In the lens, the Kruskal-Wallace test showed significant differences among the groups of G8+/TUNEL− ($P = 0.002$), G8+/TUNEL+ ($P = 0.002$), and G8−/TUNEL+ cells ($P < 0.001$). The Dunn's test revealed significant differences between the numbers of G8+/TUNEL− and G8+/TUNEL+ cells for BSS versus 18 μM G8:3DNA:Dox ($P = 0.016$ and 0.002, respectively). Significant differences also were found between the numbers of G8−/TUNEL+ cells: 36 μM G8:3DNA:Dox versus 9 μM ($P = 0.012$), 18 μM ($P = 0.006$), and 36 μM ($P = 0.006$) Dox. The Tukey's test revealed a significant difference between the number of G8+/TUNEL+ cells in lenses treated with 18 and 36 μm G8:3DNA:Dox ($P = 0.03$).

‡ In the ciliary processes, the Kruskal-Wallace test showed significant differences among the groups of G8+/TUNEL+ (0.01) and G8−/TUNEL+ cells ($P < 0.001$). No significant differences were found among the groups of G8+/TUNNEL− cells ($P = 0.38$) or between pairs of G8+/TUNEL+ cells with the Dunn's test. Significant differences were found between the numbers of G8−/TUNEL+ cells: 18 μM Dox versus 18 μM ($P = 0.024$) and 36 μM ($P = 0.009$) G8:3DNA:Dox; 36 μM Dox versus 9 μM ($P = 0.025$), 18 μM ($P = 0.014$), and 36 μM ($P = 0.006$) G8:3DNA:Dox.

§ In the cornea, no significant difference in the groups of G8+/TUNEL− cells were found with the Kruskal-Wallace test ($P = 0.079$). Significant differences were found among the groups of G8+/TUNEL+ and G8−/TUNEL+ cells ($P < 0.001$). The Dunn's test revealed significant differences between the numbers of G8+/TUNEL+ cells: 36 μM Dox versus BSS ($P = 0.024$) and 9 μM ($P = 0.041$), 18 μM ($P = 0.031$), and 36 μM ($P = 0.041$) G8:3DNA:Dox. Significant differences also were found between G8−/TUNEL+ cells: 36 μM Dox versus 9 and 36 μM ($P = 0.04$) G8:3DNA:Dox.

‖ One section without lens tissue.

¶ Values are from eight sections; one section with >25% G8−/TUNEL+ cells.

Values are from four sections; three sections with >50% G8−/TUNEL+ cells.

Effects of Drug Treatment on ACO and Soemmering's Ring Formation

ACO, when present, ranged from trace to mild by slit lamp analysis (not shown). None of the lenses in any treatment group had above trace levels of ACO when scored by gross observation (Supplementary Fig. S3A). Significant differences in ACO scores between treatment groups were not found, although the mean ACO scores were lower for the two highest doses of G8:3DNA:Dox and Dox than lower doses of both drugs.

Soemmering's rings were scored as the area covered by the ring multiplied by the intensity of regenerative material. The

Table 3. Percentage of Lenses With PCO

	BSS	G8:3DNA:Dox						Dox			3DNA:Dox
TX, μM Dox	0	0	0.36	1.8	3.6	9	18	36	9	18	36	36
Slit lamp PCO, No. lenses	15	6	6	6	2	5	5	12	5	5	8	6
% with 0	0	0	0	0	0	0	40	25	0	20	37.5	16.7
% with 0.5–1	20	0	16.7	0	0	40	40	41.7	60	40	37.5	66.7
% with 1.5–2	46.7	66.7	33.3	50	50	60	20	8.3	20	40	25	16.7
% with 2.5–3	26.7	16.7	50	50	50	0	0	25	20	0	0	0
% with 3.5–4	7	16.7	0	0	0	0	0	0	0	0	0	0
Central PCO, No. lenses	15	6	6	6	3	5	5	12	5	5	8	6
% with 0	0	0	0	0	0	0	60	41.7	0	40	62.5	33.3
% with 0.5–1	46.7	66.7	33.3	0	0	100	40	58.3	80	60	37.5	66.7
% with 1.5–2	20	0	16.7	16.7	33.3	0	0	0	20	0	0	0
% with 2.5–3	20	33.3	50	83.3	66.7	0	0	0	0	0	0	0
% with 3.5–4	13.3	0	0	0	0	0	0	0	0	0	0	0
Peripheral PCO, No. lenses	15	6	6	6	3	5	5	12	5	5	8	6
% with 0	0	0	0	0	0	0	40	33	0	20	37.5	33.3
% with 0.5–1	13.3	0	16.7	0	0	60	40	50	60	40	37.5	33.3
% with 1.5–2	33.3	66.7	16.7	0	66.7	40	20	8.3	20	40	25	16.7
% with 2.5–3	33.3	16.7	33.3	50	33.3	0	0	8.3	20	0	0	16.7
% with 3.5–4	20	16.7	33.3	50	0	0	0	0	0	0	0	0

PCO was scored by slit lamp examination. Central and peripheral PCO were scored by gross observation. The values are the percentage of total lenses scored (No. of lenses) with PCO scores of 0 = none; 0.5 to 1 = trace; 1.5 to 2.0 = mild; 2.5 to 3.0 = moderate; and 3.5 to 4.0 = severe. TX, treatment.

Investigative Ophthalmology & Visual Science

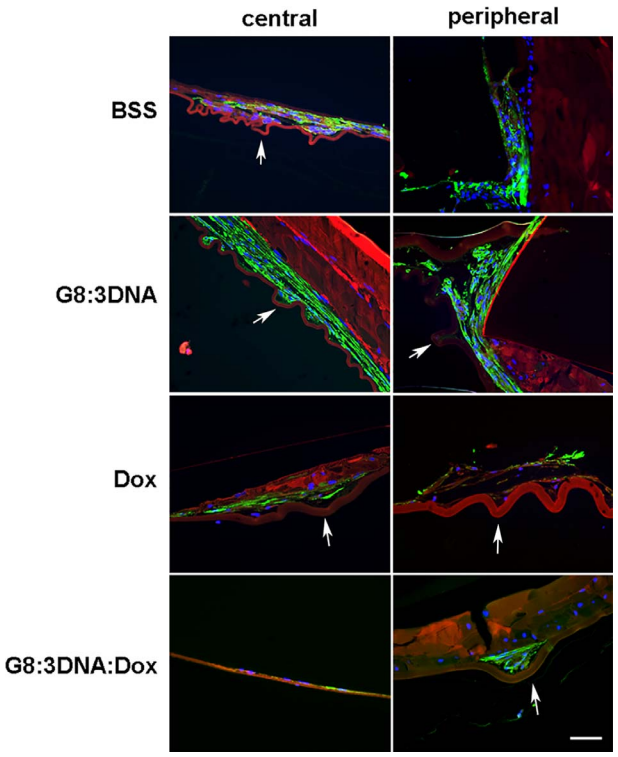

FIGURE 2. Myofibroblasts and capsular wrinkles in the lens 28 days post cataract surgery. Tissue sections of lenses treated with BSS or 36 μM Dox and G8:3DNA:Dox were double labeled with antibodies to G8 (*red*) and α-SMA (*green*). Nuclei were labeled with Hoechst dye (*blue*). Photographs were taken of the central region of posterior capsule approximately 3 mm behind the optic and peripheral posterior capsule extending from the optic-haptic junction posteriorly. *Arrows* illustrate wrinkles in the posterior capsule. *Scale bar*: 27 μM.

greatest reductions in the means from BSS, G8:3DNA, and low doses of G8:3DNA:Dox occurred in lenses treated with the two highest doses of G8:3DNA:Dox and Dox (Supplementary Fig. S3B). Significant differences were found between BSS and 18 μM G8:3DNA:Dox and Dox, and 1.8 μM G8:3DNA:Dox and 18 μM G8:3DNA:Dox and Dox. These results demonstrated that drug treatment reduces Soemmering's rings.

Analyses of Myo/Nog Cells and Myofibroblasts 4 Weeks After Cataract Surgery

Tissue sections of the anterior segment were labeled with antibodies to G8 and α-SMA 1 month after surgery to detect myofibroblasts. In the lens, no significant differences were found between the numbers of G8+/α-SMA− cells or G8−/α-SMA+ cells among the treatment groups (Table 4). However, the numbers of G8+/α-SMA+ cells did differ between treatments. Significantly fewer G8+/α-SMA+ cells were present in lenses administered G8:3DNA:Dox than BSS or G8:3DNA. By contrast, treatment with Dox or 3DNA:Dox did not significantly reduce the number of myofibroblasts in the lens compared to those injected with BSS or G8:3DNA.

G8+/α-SMA+ myofibroblasts were abundant on the central and peripheral posterior capsule (Fig. 2), in the equatorial region, and occasionally on the anterior capsule in lenses treated with BSS and G8:3DNA. Lenses administered Dox and 3DNA:Dox also contained myofibroblasts on the central and peripheral regions of the posterior capsule and in anterior and equatorial regions. G8+/α-SMA+ and G8−/α-SMA+ cells overlaid wrinkles in the capsule that were more pronounced under large aggregates of myofibroblasts than single or small clusters of these cells (Fig. 2). Wrinkles were either absent or less pronounced in lenses administered G8:3DNA:Dox than the other treatment groups.

G8+ cells were present outside of the lens in all treatment groups (Table 4). A small subpopulation of G8+ cells in the ciliary processes were α-SMA+ except in eyes administered BSS or 0.36, 1.8, 9, and 18 μM G8:3DNA:Dox. The number of G8+/α-SMA+ cells was significantly greater in 3DNA:Dox-treated eyes than BSS, all doses of G8:3DNA:Dox, and two lowest doses of Dox. G8+/α-SMA+ cells were rarely found in the cornea. No G8−/α-SMA+ cells were detected in either the ciliary processes or cornea outside of blood vessels in any of the treatment groups.

In summary, double labeling with G8 and α-SMA antibodies revealed that treatment with G8:3DNA:Dox significantly reduced the number of myofibroblasts in the lens. The targeting drug also reduced wrinkles in the lens capsule. While Myo/Nog cells were present in the ciliary processes and cornea, these structures contained few, if any, myofibroblasts except in eyes treated with 3DNA:Dox.

Effects of Drug Treatment on Corneal Edema and Cell Viability 4 Weeks After Cataract Surgery

Analyses of corneal edema by slit lamp examination on weeks 1 to 4 are displayed in Supplementary Text and Table S2. Gross observation and histologic assessment on day 28 revealed that the anterior chambers were clear and deep, irises and peripheral retinas appeared normal, and the trabecular meshworks were open in all eyes (Fig. 3). One rabbit exhibited barely detectable corneal edema in the eye treated with 36 μM G8:3DNA:Dox and a trace level of corneal edema in the eye with the same dose of Dox.

The results of TUNEL staining in the lens 28 days after surgery are displayed in Figure 3 and Table 5. Lenses treated with the highest dose of G8:3DNA:Dox contained significantly fewer G8+/TUNEL− cells than those administered BSS, G8:3DNA, 3DNA:Dox, and 9 and 36 μM Dox. The population of G8+/TUNEL+ cells was statistically similar among the treatment groups. G8−/TUNEL+ cells were few in number in BSS-, G8:3DNA-, and G8:3DNA:Dox-treated lenses, and significantly less abundant in the 18 μM G8:3DNA:Dox lenses than those injected with the same dose of Dox or 3DNA:Dox.

In the ciliary processes, the numbers of G8+/TUNEL− and G8+/TUNEL+ cells were statistically similar in all treatment groups (Table 5). By contrast, the population of G8−/TUNEL+ cells was significantly elevated in eyes administered BSS, G8:3DNA, Dox (9 and 36 μM), and 3DNA:Dox compared to the two highest doses of G8:3DNA:Dox. The cornea exhibited significantly more of G8+/TUNEL− and G8−/TUNEL+ cells in eyes treated with 36 μM Dox and 3DNA:Dox than the three highest doses of G8:3DNA:Dox. Dying epithelial and stromal cells were mostly concentrated in the peripheral cornea (Fig. 3).

In summary, fewer Myo/Nog cells were present in lenses administered the highest dose of G8:3DNA:Dox than the other treatment groups. Few cells were dying in the lens except in those treated with the second highest dose of Dox and 3DNA:Dox. Treatment with Dox and 3DNA:Dox during cataract surgery has lasting, toxic effects in the ciliary processes and cornea.

DISCUSSION

The incidence of PCO has been reduced, but not eliminated, by more extensive removal or repositioning of lens tissue

Table 4. Expression of α-SMA in G8+ and G8− Cells in the Anterior Segment 28 Days After Cataract Surgery

	No. Eyes	No. Sect*	Lens†			CP‡			Cornea§		
			G8+/α-SMA−	G8+/α-SMA+	G8−/α-SMA+	G8+/α-SMA−	G8+/α-SMA+	G8−/α-SMA+	G8+/α-SMA−	G8+/α-SMA+	G8−/α-SMA+
BSS	13	19	3 ± 6	47 ± 37	2 ± 9	10 ± 10	0	0	3 ± 6	3 ± 7	0
G8:3DNA	6	10||	0	68 ± 11	0	5 ± 9	9 ± 8	0	2 ± 1	0	0
G8:3DNA:Dox											
0.36 μM	6	6	0.2 ± 0.4	0	0	3.2 ± 3.7	0	0	0.5 ± 0.8	0	0
1.8 μM	5	5	2 ± 6	0	0	2 ± 2	0	0	2 ± 1	0	0
3.6 μM	5	8	0.3 ± 0.7	11 ± 6	0	4 ± 2	2 ± 5	0	4 ± 1	0	0
9 μM	5	10¶	2 ± 3	4 ± 5	0	0	0	0	2 ± 1	0.1 ± 0.3	0
18 μM	5	10#	0.4 ± 1	1 ± 2	0	8 ± 5	0	0	4 ± 4	0	0
36 μM	11	18	0.4 ± 2	9 ± 13	0	11 ± 7	3 ± 5	0	3 ± 1	0	0
Dox											
9 μM	5	12	5 ± 9	27 ± 17	0**	14 ± 5	0.2 ± 1	0	11 ± 6	1 ± 5	0
18 μM	5	10	1 ± 3	18 ± 18	0	11 ± 5	0.2 ± 0.6	0	18 ± 18	0.2 ± 0.6	0
36 μM	9	14	0	35 ± 17	0	5 ± 7	4 ± 7	0	7 ± 6	1 ± 2	0
3DNA:Dox											
36 μM	6	11	0.1 ± 0.3	57 ± 12	1 ± 2	2 ± 5	15 ± 7	0	3 ± 1	0	0

* Tissue sections were double labeled with antibodies to G8 and α-SMA. The results are the mean ± standard deviation of the number of cells in the lens, CP, and cornea labeled with G8 only (G8+/α-SMA−), both G8 and α-SMA (G8+/α-SMA+), or α-SMA only (G8−/α-SMA+).

† In the lens, Kruskal-Wallis test showed P values of 0.01 and <0.001 for the groups of G8+/α-SMA− and G8+/α-SMA+ cells, respectively, but no differences among the group for the G8−/TUNEL+ cells. No significant differences were found between pairs of G8+/α-SMA− cells. Significant differences were found between the numbers of G8+/α-SMA+ cells by the Dunn's test: BSS versus 0.36 μM (P = 0.008), 6 μM (P = 0.023), and 18 μM (P = 0.008) G8:3DNA:Dox; G8:3DNA (0 Dox) versus 0.36, 1.8, 18, 36 μM ($P < 0.001$) and 9 μM (P = 0.005) G8:3DNA:Dox; 3DNA:Dox (36 μM) versus 0.36, 1.8, 18, 36 μM ($P < 0.001$) and 9 μM (P = 0.008) G8:3DNA:Dox.

‡ In the ciliary body, the Dunn's test revealed significant differences between the number of G8+/α-SMA− cells: 3DNA:Dox versus 17.5 μM (P = 0.001) and 35 μM (P = 0.002) Dox, BSS (P = 0.01), and 35 μM (P = 0.032) and 36 μM ($P < 0.001$) G8:3DNA:Dox. Significant differences also were found in the numbers of G8+/ α-SMA+ cells: 3DNA:Dox versus 0.36, 1.8, 9, 18, and 36 μM G8:3DNA:Dox (P = 0.018, 0.04, 0.002, 0.002, and 0.04, respectively), 9 μM (P = 0.002) and 18 μM (P = 0.006) Dox, and BSS ($P < 0.0.001$). No significant differences were found in the numbers of G8−/α-SMA+ cells (P = 1).

§ In the cornea, significant differences were found in the numbers of G8+/α-SMA− cells: 9 μM Dox versus 0.36 μM (P = 0.001) and 1.8 μM ($P < 0.001$) G8:3DNA:Dox, and BSS ($P < 0.001$); and 18 μM Dox versus 0.36 and 1.8 μM G8:3DNA:Dox and BSS ($P < 0.001$). No significant differences were found in the numbers of G8+/SMA+ (P = 0.24) or G8−/α-SMA− cells (P = 1) in the cornea.

|| Four sections without lens tissue.

¶ Two sections without lens cells.

One section without lens tissue.

** Value is from seven sections; two sections with >50% G8−/α-SMA+ cells.

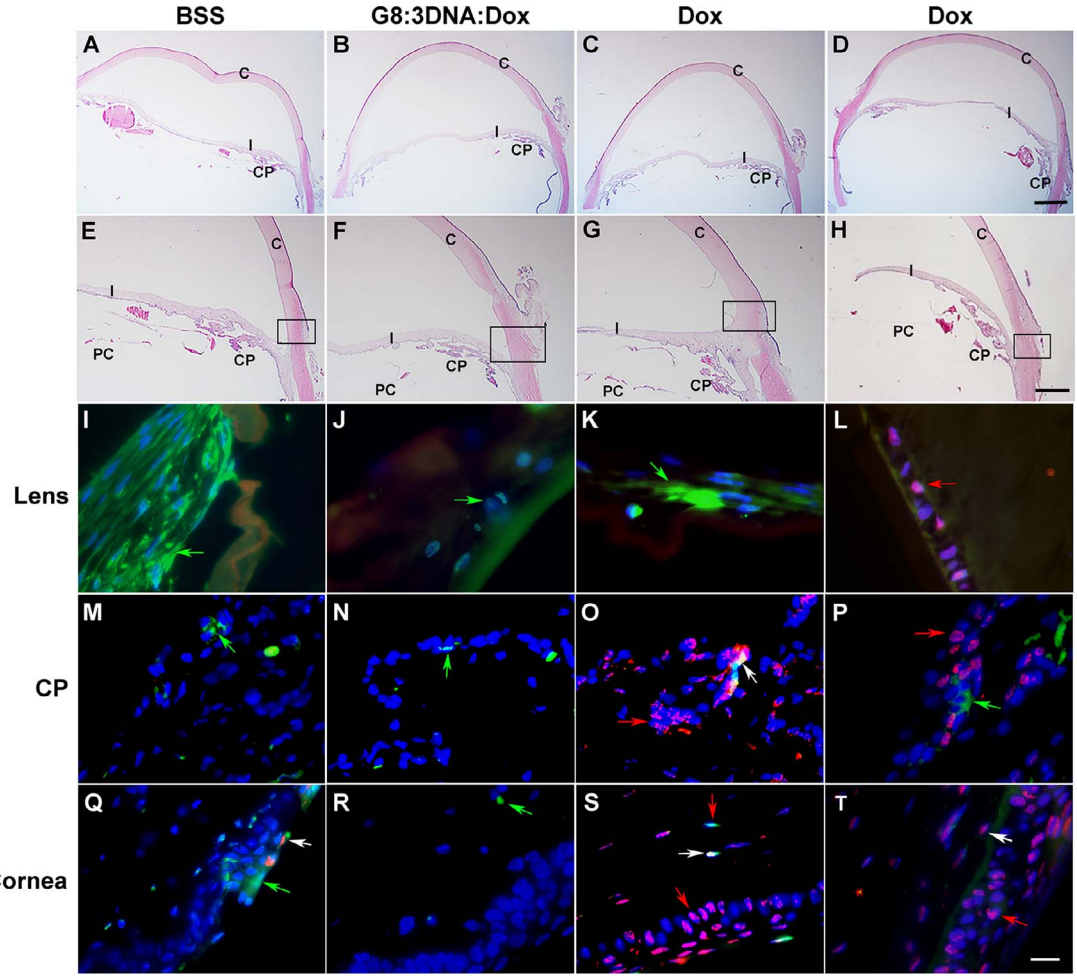

Figure 3. Effects of drug treatment 4 weeks after cataract surgery. Lenses were injected with BSS, 36 μM G8:3DNA:Dox, 36 μM Dox (**C**, **G**, **K**, **O**, **S**), or 9 μM Dox (**D**, **L**, **P**, **T**) during cataract surgery. Four weeks later, tissue sections were stained with H&E (**A–H**) or double labeled with the G8 mAb (*green*) and TUNEL reagents (*red*) (**I–T**). Overlap of *red* and *green* appears *yellow* in merged images. Nuclei were labeled with Hoechst dye (*blue*). *Boxes* in (**E–H**) are shown at high magnification in (**Q–T**). *White arrows* = G8+/TUNEL+ cells; *green arrows* = G8+/TUNEL– cells; *red arrows* = G8–/TUNEL+ cells. *Bar*: 540 μM in (**A–D**), 270 in (**E–H**), and 9 μM in (**I–T**). C, cornea; CP, ciliary processes; I, iris.

during surgery, advances in the composition and conformation of IOLs, and posterior capsulorhexis.[8,13,44–49] While certain drugs may impede the initial response of cells to surgery, it is uncertain whether they would continue to block development of PCO that may arise months or years later.[13,20,50–52] Cytotoxic drugs and chemicals that nonspecifically kill cells at the time of surgery and extensive removal of lens epithelial cells may cause the IOL to be more mobile, and drugs may diffuse to surrounding ocular tissues and initiate an inflammatory response to necrotic tissue.[47,53–58] Currently, there is no effective method for predicting who will develop PCO or preventing its occurrence, and eradication of the disease remains an unmet goal in ophthalmology. Prevention of PCO is particularly important for insertion of shape-changing IOLs that accommodate for distance because fibrosis and contractions affect the flexibility of the lens capsule.[59]

In this study, we built upon our proof-of-concept experiments demonstrating that G8:3DNA:Dox prevents the emergence of myofibroblasts in explant cultures of human lens tissue.[33] The model we used to examine the drug's effect on development of PCO in vivo was the adult rabbit that develops the disease within a month of cataract surgery, the approximate equivalent of 2 years in humans.[60] The percentage of adult rabbits that developed clinically significant PCO resembles the high incidence of PCO in children who have undergone cataract surgery.[60] Thus, the rabbit is an aggressive model of PCO formation that presents a significant challenge for testing potential therapeutics.

Administration of G8:3DNA:Dox into the lens specifically targeted Myo/Nog cells in the lens with minimal, if any, off-target effects in the ciliary body and cornea during the first 48 hours following cataract surgery. By contrast, off-target effects were observed 2 days after treatment with Dox that killed both Myo/Nog and lens epithelial cells, as well as cells in the ciliary processes and cornea. Dox also displayed adverse effects in the cornea and ciliary processes 4 weeks after surgery, well after the expected rate of drug elimination via the flow of aqueous humor.[61] Diffusion of Dox to surrounding tissues may lead to a chronic, inflammatory wound environment in which cell death continues in the absence of the original insult.

Targeted depletion of Myo/Nog cells in the lens with G8:3DNA:Dox reduced PCO and Soemmering's rings, myofibroblasts, and wrinkles in the lens capsule without apparent off-target effects in other structures of the anterior segment 4 weeks after surgery. Doses of G8:3DNA:Dox containing 9 to 36 μM Dox prevented central PCO from developing above trace levels. Fewer than 9% of lenses administered these doses of G8:3DNA:Dox exhibited greater than mild levels of peripheral

Table 5. Cell Death in the Anterior Segment 28 Days After Cataract Surgery

	No. Eyes	No. Sect*	Lens†			CP‡			Cornea§		
			G8+/TUN−	G8+/ TUN+	G8−/ TUN+	G8+/ TUN−	G8+/ TUN+	G8−/ TUN+	G8+/ TUN−	G8+/ TUN+	G8−/ TUN+
Unoperated	2	6	4 ± 1	0	0	4 ± 2	0	0.2 ± 0.4	5 ± 1	0	5 ± 2
BSS	8	16	55 ± 3	0	0	12 ± 4	0.1 ± 0.25	7 ± 5	13 ± 5	0	8 ± 3
G8:3DNA	5	10	44 ± 15	1 ± 1	1 ± 1	8 ± 2	0	1 ± 2	8 ± 3	0	7 ± 1
G8:3DNA:Dox											
9 μM	5	10	12 ± 8	6 ± 12	1 ± 3	12 ± 4	0	1 ± 1	7 ± 2	0	2 ± 2
18 μM	5	9	11 ± 10	5 ± 10	0	10 ± 5	1 ± 2	5 ± 10	7 ± 2	5 ± 11	1 ± 1||
36 μM	7	14	2 ± 3	1 ± 3	0.4 ± 1	7 ± 5	0	0.2 ± 0.4	6 ± 2	0	4 ± 3
Dox											
9 μM	4	8	33 ± 28	3 ± 2	11 ± 14	11 ± 4	2 ± 2	18 ± 17	12 ± 4	4 ± 10	17 ± 10¶
18 μM	5	9	14 ± 14	15 ± 25	8 ± 8||	12 ± 7	3 ± 5	13 ± 15||	10 ± 7	7 ± 8	19 ± 20||
36 μM	6	13	29 ± 10	1 ± 3	2 ± 4	10 ± 4	1 ± 2	19 ± 15	16 ± 5	2 ± 2	43 ± 25
3DNA:Dox											
36 μM	5	10	30 ± 12	5 ± 5	11 ± 9	14 ± 6	0.1 ± 0.3	17 ± 14	20 ± 5	2 ± 2	47 ± 17#

* Tissue sections (Sect) were double labeled with the G8 mAb and TUNEL (TUN) reagents to detect cell death. The results are the mean ± standard deviation of the number of cells in the lens, CP, and cornea labeled for G8 only (G8+/TUN−), both G8 and TUNEL (G8+/TUN+), or TUNEL only (G8−/TUN+).

† In the lens, Kruskal-Wallace test showed significant differences among the groups of G8+/TUNEL− ($P < 0.001$), G8+/TUNEL+ ($P = 0.04$), and G8−/TUNEL+ cells ($P < 0.001$). Significant differences in pairs were not found for G8+/TUNEL+ cells by the Dunn's test. Significant differences were found between the numbers of G8+/TUNEL− cells: G8:3DNA versus 9 ($P < 0.001$), 18 ($P = 0.016$), and 36 μM ($P = 0.019$) G8:3DNA:Dox and 18 μM Dox ($P = 0.036$); 3DNA:Dox versus 36 μM G8:3DNA:Dox ($P < 0.001$); and 36 μM G8:3DNA:Dox versus BSS ($P < 0.001$) and 9 μM ($P = 0.006$) and 36 μM ($P < 0.001$) Dox. Significant differences also were found between the numbers of G8−/TUNEL+ cells: 18 μM G8:3DNA:Dox versus 18 μM Dox ($P = 0.034$) and 36 μM 3DNA:Dox ($P = 0.018$).

‡ In the ciliary body, the Kruskal-Wallace test revealed significant differences among the groups of G8+/TUNEL− ($P = 0.013$), G8+/TUNEL+ ($P = 0.004$), and G8−/TUNEL+ cells ($P < 0.001$). No significant differences were present among the pairs of G8+/TUNEL− and G8+/TUNEL+ cells by the Dunn's test. Significant differences were found between the numbers of G8−TUNEL+ cells: 36 μM G8:3DNA:Dox versus BSS ($P = 0.033$), 9 μM ($P = 0.023$) and 36 μM ($P < 0.001$) Dox; 36 μM Dox versus G8:3DNA ($P = 0.027$) and 9 μM G8:3DNA:Dox ($P = 0.006$); and 3DNA:Dox versus 9 μM G8:3DNA:Dox ($P = 0.027$).

§ In the cornea, the Kruskal-Wallace test showed significant differences among the groups of G8+/TUNEL−, G8+/TUNEL+, and G8−/TUNEL+ cells ($P < 0.001$). The Dunn's test showed significant differences between the numbers of G8+/TUNEL− cells: 36 μM Dox versus 9 ($P = 0.03$), 18 ($P = 0.025$), and 36 μM ($P < 0.001$) G8:3DNA:Dox ($P < 0.001$), and 3DNA:Dox versus 9 to 36 μM G8:3DNA:Dox ($P < 0.001$). No significant differences were found between the pairs for G8+/TUNEL+ cells. Significant differences were present between pairs of G8−/TUNEL+ cells: 36 μM Dox and 3DNA:Dox versus 9 to 36 μM G8:3DNA:Dox ($P < 0.001$).

|| Values are from seven sections; two sections had >50% G8−/TUNEL+ cells.

¶ Value is from four sections; four sections had >50% G8−/TUNEL+/ cells.

Value is from eight sections; two sections had >20% G8−/TUNEL+/ cells.

PCO. Administration of the drug as a sustained delivery formulation may reduce the incidence of PCO even further and protect the lens from Myo/Nog cells that migrate on the zonule fibers from the ciliary processes to the lens[36] (Gerhart JV, et al. *IOVS* 2017;58:ARVO E-Abstract 3635). The modularity of the 3DNA platform, as well as the wide range of available conjugation chemistries, allows for the direct attachment of a variety of small drugs. Thus, additional cytotoxins conjugated to G8:3DNA can be tested for their effects on PCO.

Injection of Dox and 3DNA:Dox into the lens illustrated that indiscriminate killing of cells in the lens also reduces PCO. Dox may decrease the number of lens epithelial and Myo/Nog cells available to migrate onto the posterior capsule. It is also possible that remaining Myo/Nog cells respond to cell death induced by Dox in the equatorial region and differentiate into syncytia of myofibroblasts that create a barrier to posterior migration. Precedence for this interpretation comes from our previous study demonstrating that Myo/Nog cells rapidly migrate to a subpopulation of dying cells in the early embryo.[30]

Whereas treatment with G8:3DNA:Dox significantly reduced the population of myofibroblasts in the lens, no difference in the number of these contractile cells was observed between Dox- and BSS-treated lenses. Myofibroblasts overlaid wrinkles in the lens capsule. Distortions in the central region of the posterior capsule are expected to affect visual acuity by diffracting light; however, contractions occurring in the peripheral portion of the posterior capsule also may impact the visual axis.

The value of drugs that target a specific population lies in their reduced side effects, as illustrated with the depletion of Myo/Nog cells in the lens. Injection of drugs into the lens during cataract surgery would minimally increase time in the operating room. However, the synthesis of conjugates that specifically deliver a cytotoxin to a tissue, or in the case of the lens, the progenitors of myofibroblasts, is a more complex, time-consuming, and costly process than production of a cytotoxin alone. The return on the investment of conjugate synthesis and administration is a potential savings of hundreds of millions of dollars spent each year to treat PCO and the side effects of laser therapy, and most importantly, preservation of vision.

Acknowledgments

Supported by the Sharpe – Strumia Research Foundation (SSRF2010-2015) (MG-W), an anonymous donation for the Myo/Nog cell program project (MG-W, JG, AB-N), and an unrestricted grant from Research to Prevent Blindness, Inc, New York, New York, United States, to the Department of Ophthalmology and Visual Sciences, University of Utah (LW, NM).

Disclosure: **J. Gerhart**, P; **L. Werner**, None; **N. Mamalis**, None; **J. Infanti**, None; **C. Withers**, None; **F. Abdalla**, None; **C. Gerhart**, None; **A. Bravo-Nuevo**, None; **O. Gerhart**, None; **L. Getts**, Genisphere, LLC (E); **K. Rhodes**, Genisphere, LLC (E); **J. Bowers**, Genisphere, LLC (E); **R. Getts**, Genisphere, LLC (I, E, S), P; **M. George-Weinstein**, P

References

1. Harding JJ. *Cataract: Biochemistry, Epidemiology and Pharmacology*. London: Chapman and Hall; 1991.
2. Vision 2020: the cataract challenge. *Community Eye Health*. 2000;13:17–19.
3. Brian G, Taylor H. Cataract blindness—challenges for the 21st century. *Bull World Health Organ*. 2001;79:249–256.
4. Sharma N, Pushker N, Dada T, Vajpayee RB, Dada VK. Complications of pediatric cataract surgery and intraocular lens implantation. *J Cataract Refract Surg*. 1999;25:1585–1588.
5. Baratz KH, Cook BE, Hodge DO. Probability of Nd:YAG laser capsulotomy after cataract surgery in Olmsted County, Minnesota. *Am J Ophthalmol*. 2001;131:161–166.
6. Boureau C, Lafuma A, Jeanbat V, Smith AF, Berdeaux G. Cost of cataract surgery after implantation of three intraocular lenses. *Clin Ophthalmol*. 2009;3:277–285.
7. Apple DJ, Solomon KD, Tetz MR, et al. Posterior capsule opacification. *Surv Ophthalmol*. 1992;37:73–116.
8. Awasthi N, Guo S, Wagner BJ. Posterior capsular opacification: a problem reduced but not yet eradicated. *Arch Ophthalmol*. 2009;127:555–562.
9. Moisseiev J, Bartov E, Schochat A, Blumenthal M. Long-term study of the prevalence of capsular opacification following extracapsular cataract extraction. *J Cataract Refract Surg*. 1989;15:531–533.
10. Findl O, Menapace R. PCO still a major hurdle in successful cataract surgery. *Ocular Surgery News Europe Edition*. May 2011.
11. Sabbagh L. PCO: what's wrong with doing a YAG? *Review of Ophthalmology*. May 10, 2018.
12. Busbee BG, Brown GC, Brown MM. Cost-effectiveness of ocular interventions. *Curr Opin Ophthalmol*. 2003;14:132–138.
13. Wormstone IM, Wang L, Liu CS. Posterior capsule opacification. *Exp Eye Res*. 2009;88:257–269.
14. Raj SM, Vasavada AR, Joar K, Vasavada VA, Vasavada VA. Postoperative capsular opacification: a review. *Int J Biomed Sci*. 2007;3:13.
15. Kappelhof JP. The ring of soemmerring in man: an ultrastructural study. *Graefes Arch Clin Exp Ophthalmol*. 1983;225:77–83.
16. Shu DY, Lovicu FJ. Myofibroblast transdifferentiation: the dark force in ocular wound healing and fibrosis. *Prog Retin Eye Res*. 2017;60:44–65.
17. McDonnell PJ, Zarbin MA, Green WR. Posterior capsule opacification in pseudophakic eyes. *Ophthalmology*. 1983;90:1548–1553.
18. Wormstone IM, Tamiya S, Anderson I, Duncan G. TGF-beta2-induced matrix modification and cell transdifferentiation in the human lens capsular bag. *Invest Ophthalmol Vis Sci*. 2002;43:2301–2308.
19. Wormstone IM, Tamiya S, Eldred JA, et al. Characterisation of TGF-beta2 signalling and function in a human lens cell line. *Exp Eye Res*. 2004;78:705–714.
20. Wormstone IM, Anderson IK, Eldred JA, Dawes LJ, Duncan G. Short-term exposure to transforming growth factor beta induces long-term fibrotic responses. *Exp Eye Res*. 2006;83:1238–1245.
21. Dawes LJ, Eldred JA, Anderson IK, et al. TGF beta-induced contraction is not promoted by fibronectin-fibronectin receptor interaction, or alpha SMA expression. *Invest Ophthalmol Vis Sci*. 2008;49:650–661.
22. Gerhart J, Baytion M, DeLuca S, et al. DNA dendrimers localize MyoD mRNA in presomitic tissues of the chick embryo. *J Cell Biol*. 2000;149:825–834.
23. Gerhart J, Neely C, Stewart B, et al. Epiblast cells that express MyoD recruit pluripotent cells to the skeletal muscle lineage. *J Cell Biol*. 2004;164:739–746.
24. Gerhart J, Elder J, Neely C, et al. MyoD-positive epiblast cells regulate skeletal muscle differentiation in the embryo. *J Cell Biol*. 2006;175:283–292.
25. Strony R, Gerhart J, Tornambe D, et al. NeuroM and MyoD are expressed in separate subpopulations of cells in the pregastrulating epiblast. *Gene Expr Patterns*. 2005;5:387–395.

26. George-Weinstein M, Gerhart J, Reed R, et al. Skeletal myogenesis: the preferred pathway of chick embryo epiblast cells in vitro. *Dev Biol*. 1996;173:279–291.
27. Gerhart J, Neely C, Elder J, et al. Cells that express MyoD mRNA in the epiblast are stably committed to the skeletal muscle lineage. *J Cell Biol*. 2007;178:649–660.
28. Gerhart J, Pfautz J, Neely C, et al. Noggin producing, MyoD-positive cells are crucial for eye development. *Dev Biol*. 2009; 336:30–41.
29. Gerhart J, Bast B, Neely C, et al. MyoD-positive myoblasts are present in mature fetal organs lacking skeletal muscle. *J Cell Biol*. 2001;155:381–392.
30. Gerhart J, Scheinfeld VL, Milito T, et al. Myo/Nog cell regulation of bone morphogenetic protein signaling in the blastocyst is essential for normal morphogenesis and striated muscle lineage specification. *Dev Biol*. 2011;359:12–25.
31. Gerhart J, Hayes C, Scheinfeld V, Chernick M, Gilmour S, George-Weinstein M. Myo/Nog cells in normal, wounded and tumor bearing skin. *Exp Dermatol*. 2012;21:466–468.
32. Gerhart J, Greenbaum M, Scheinfeld V, et al. Myo/Nog cells: targets for preventing the accumulation of skeletal muscle-like cells in the human lens. *PLoS One*. 2014;9:e95262.
33. Gerhart J, Greenbaum M, Casta L, et al. Antibody-conjugated, DNA-based nanocarriers intercalated with doxorubicin eliminate myofibroblasts in explants of human lens tissue. *J Pharmacol Exp Ther*. 2017;361:60–67.
34. Brandli A, Gerhart J, Sutera CK, et al. Role of Myo/Nog Cells in neuroprotection: evidence from the light damaged retina. *PLoS One*. 2017;12:e0169744.
35. Bravo-Nuevo A, Brandli AA, Gerhart J, et al. Neuroprotective effect of Myo/Nog cells in the stressed retina. *Exp Eye Res*. 2016;146:22–25.
36. Gerhart J, Withers C, Gerhart C, et al. Myo/Nog cells are present in the ciliary processes, on the zonule of Zinn and posterior capsule of the lens following cataract surgery. *Exp Eye Res*. 2018;171:101–105.
37. Walker JL, Zhai N, Zhang L, et al. Unique precursors for the mesenchymal cells involved in injury response and fibrosis. *Proc Natl Acad Sci U S A*. 2010;107:13730–13735.
38. Li J, Werner L, Guan JJ, Reiter N, Mamalis N. Evaluation of long-term biocompatibility and capsular bag opacification with a new silicone-polyimide plate-type intraocular lens in the rabbit model. *J Cataract Refract Surg*. 2016;42:1066–1072.
39. Kramer GD, Werner L, MacLean K, Farukhi A, Gardiner GL, Mamalis N. Evaluation of stability and capsular bag opacification with a foldable intraocular lens coupled with a protective membrane in the rabbit model. *J Cataract Refract Surg*. 2015; 41:1738–1744.
40. Bozukova D, Werner L, Mamalis N, et al. Double-C loop platform in combination with hydrophobic and hydrophilic acrylic intraocular lens materials. *J Cataract Refract Surg*. 2015;41:1490–1502.
41. Werner L, Pandey SK, Apple DJ, Escobar-Gomez M, McLendon L, Macky TA. Anterior capsule opacification: correlation of pathologic findings with clinical sequelae. *Ophthalmology*. 2001;108:1675–1681.
42. Werner L, Mamalis N, Izak AM, et al. Posterior capsule opacification in rabbit eyes implanted with 1-piece and 3-piece hydrophobic acrylic intraocular lenses. *J Cataract Refract Surg*. 2005;31:805–811.
43. Nishi O, Nishi K. Preventing posterior capsule opacification by creating a discontinuous sharp bend in the capsule. *J Cataract Refract Surg*. 1999;25:521–526.
44. Davison JA. Neodymium:YAG laser posterior capsulotomy after implantation of AcrySof intraocular lenses. *J Cataract Refract Surg*. 2004;30:1492–1500.
45. Pepose JS, Hayashida J, Hovanesian J, et al. Safety and effectiveness of a new toric presbyopia-correcting posterior chamber silicone intraocular lens. *J Cataract Refract Surg*. 2015;41:295–305.
46. Nibourg LM, Gelens E, Kuijer R, Hooymans JM, van Kooten TG, Koopmans SA. Prevention of posterior capsular opacification. *Exp Eye Res*. 2015;136:100–115.
47. Nishi O, Nishi K, Osakabe Y. Effect of intraocular lenses on preventing posterior capsule opacification: design versus material. *J Cataract Refract Surg*. 2004;30:2170–2176.
48. Green WT, Boase DL. How clean is your capsule? *Eye (Lond)*. 1989;3:678–684.
49. Menapace R. Posterior capsulorhexis combined with optic buttonholing: an alternative to standard in-the-bag implantation of sharp-edged intraocular lenses: a critical analysis of 1000 consecutive cases. *Graefes Arch Clin Exp Ophthalmol*. 2008;246:787–801.
50. Laurell CG, Zetterstrom C. Effects of dexamethasone, diclofenac, or placebo on the inflammatory response after cataract surgery. *Br J Ophthalmol*. 2002;86:1380–1384.
51. Flach AJ, Dolan BJ. Incidence of postoperative posterior capsular opacification following treatment with diclofenac 0.1% and ketorolac 0.5% ophthalmic solutions: 3-year randomized, double-masked, prospective clinical investigation. *Trans Am Ophthalmol Soc*. 2000;98:101–105.
52. Walker JL, Wolff IM, Zhang L, Menko AS. Activation of SRC kinases signals induction of posterior capsule opacification. *Invest Ophthalmol Vis Sci*. 2007;48:2214–2223.
53. Ohguro N, Fukuda M, Sasabe T, Tano Y. Concentration dependent effects of hydrogen peroxide on lens epithelial cells. *Br J Ophthalmol*. 1999;83:1064–1068.
54. Fernandez V, Fragoso MA, Billotte C, et al. Efficacy of various drugs in the prevention of posterior capsule opacification: experimental study of rabbit eyes. *J Cataract Refract Surg*. 2004;30:2598–2605.
55. Liu H, Feng G, Wu L, et al. The effects of rapamycin on lens epithelial cell proliferation, migration, and matrix formation: an in vitro study. *Mol Vis*. 2010;16:1646–1653.
56. Huang X, Wang Y, Cai JP, et al. Sustained release of 5-fluorouracil from chitosan nanoparticles surface modified intra ocular lens to prevent posterior capsule opacification: an in vitro and in vivo study. *J Ocul Pharmacol Ther*. 2013;29: 208–215.
57. Spalton DJ, Russell SL, Evans-Gowing R, Eldred JA, Wormstone IM. Effect of total lens epithelial cell destruction on intraocular lens fixation in the human capsular bag. *J Cataract Refract Surg*. 2014;40:306–312.
58. D'Antin JC, Barraquer RI, Tresserra F, Michael R. Prevention of posterior capsule opacification through intracapsular hydrogen peroxide or distilled water treatment in human donor tissue. *Sci Rep*. 2018;8:12739.
59. Alio JL, Alio Del Barrio JL, Vega-Estrada A. Accommodative intraocular lenses: where are we and where we are going. *Eye Vis (Lond)*. 2017;4:16.
60. Gwon A. The rabbit in cataract/IOL surgery. *Anim Models Eye Res*. 2008;184–203.
61. Johnson F, Maurice D. A simple method of measuring aqueous humor flow with intravitreal fluoresceinated dextrans. *Exp Eye Res*. 1984;39:791–805.

Investigative Ophthalmology & Visual Science